JPP Journal of Pharmacy and Pharmacology

Journal of Pharmacy and Pharmacology, 2021, Vol 73, 410–423
doi:10.1093/jpp/rgaa044
Research Paper
Advance Access publication 8 February 2021

OXFORD

Research Paper

Glochidion ellipticum Wight extracts ameliorate dextran sulfate sodium-induced colitis in mice by modulating nuclear factor kappa-light-chain-enhancer of activated B cells signalling pathway

Imam Hossen[1,2,3], Wu Hua[1,5], Arshad Mehmood[1,2,3], Rifat Nowshin Raka[1,2,3], Song Jingyi[1], Jin Jian-Ming[1,5], Xu Min[1,2,3], Ashbala Shakoor[1,2,4], Cao Yanping[1,2], Chengtao Wang[1,2,3] and Xiao Junsong[1,2,3,*]

[1]Beijing Technology and Business University, Beijing, China
[2]Beijing Advanced Innovation Center for Food Nutrition and Human Health, Beijing, China
[3]Beijing Engineering and Technology Research Center of Food Additives, Beijing, China
[4]Beijing Laboratory for Food Quality and Safety, Beijing, China
[5]Beijing Key Lab of Plant Resource Research and Development, Beijing, China

*Correspondence: Xiao Junsong, College of food and health, Beijing Technology and Business University, Building No. 8, Fucheng Road 11#, Haidian District, Beijing 100048, China. Tel: +86-13436877820; Fax: +86-10-68984003; Email: xiaojs@th.btbu.edu.cn

Received June 9, 2020; Accepted November 13, 2020.

Abstract

Objectives *Glochidion ellipticum* Wight is a medicinal plant, rich in polyphenols, frequently used by the indigenous communities of Bangladesh and possess with multiple health benefits. It exerts anti-inflammatory and antidiarrheal properties, but the detailed chemical constituents are yet to be elucidated.

Methods *Glochidion ellipticum* extracts were analyzed using ultra-high performance liquid chromatography/quadrupole time-of-flight mass spectrometry and then tested by both lipopolysaccharide (LPS) induced inflammation of Raw 264.7 macrophage cells and dextran sulfate sodium (DSS) induced acute colitis model. Blood serum was taken for fluorescein isothiocyanate–dextran (FITC-dextran) measurement and tissue samples were used to perform histology, RT-PCR and Western blotting.

Key findings The extracts could lower the levels of nitric oxide (NO), reactive oxygen species (ROS) and pro-inflammatory cytokines significantly in LPS induced macrophage cells. The extracts could also reduce disease activity index (DAI) score, restore antioxidants and pro-oxidants and improve macroscopic and microscopic features of colonic tissues in DSS induced mice. Expression of inducible nitric oxide synthase (iNOS) and cyclooxygenase-2 (COX-2) in protein level was markedly diminished (up to 51.21% and 71.11%, respectively) in the treatment groups compared to the model group of colitic mice.

Conclusions Our findings suggested that *G. ellipticum* extracts ameliorate DSS colitis via blocking nuclear factor kappa-light-chain-enhancer of activated B cells (NF-κB) signaling pathway, which make them to be potential candidates for further research against inflammation and colitis.

Keywords: phytochemicals; *Glochidion ellipticum*; intestinal permeability; acute colitis; inflammatory bowel disease; oxidative stress

Introduction

Western and rapidly developing countries are showing the highest rate of inflammatory bowel disease (IBD) due to lifestyle changes, diet, smoking, drinking alcoholic beverages and environmental factors, etc.[1, 2] Generally, IBD is branded as the disease of western developed countries. However, recent data suggests otherwise, as many eastern countries with less development are also reporting an increasing number of cases every year.[3] The symptoms of IBD include bodyweight loss, blood in the stool, diarrhoea and abdominal cramps (Rodriguez-Canales *et al*., 2016).[4, 5] The causal factors of IBD are still up for discussion, but most agree on the overproduction of reactive oxygen species (ROS) and changes in gut microbiota composition (Rezaie *et al*., 2007).[6, 7, 8] Because of immune cell activation, the intestinal barrier can be damaged directly and indirectly by several mechanisms and all of them exclusively involve ROS.[9, 10] Moreover, ROS modulates numerous steps in inflammatory cascades by activating several pathways like Mitogen-activated protein kinases (MAPKs), and nuclear factor kappa-light-chain-enhancer of activated B cells (NF-κB), etc. These, in turn, leads to the production of pro-inflammatory cytokines and chemokines in the affected areas.[11, 12, 13]

The common drugs to treat IBD include corticosteroids, aminosalicylates, immunosuppressants and even monoclonal antibodies to target specific protein deactivation.[14, 15] Besides these, dietary agents and phytochemicals from a wide range of plants are also in use, mostly because of their easy availability, low cost and less or no toxicity.[16, 17, 18, 19, 20, 21] The reason behind this is the majority of market drugs are mostly like suppressing medication. They alleviate the disease to a certain extent and exert some complications in long run.[22, 23, 24] The quest for a convenient and precise medication of IBD is urgent. Phytochemicals from hundreds of plants are already experimented and possess the potential to be used as an alternative medication for IBD.[25, 26, 27] *Glochidion ellipticum* Wight is a medium-sized evergreen tree belonging to the Phyllanthaceae family. Previous studies suggested that the leaves of this plant are rich in flavonoids, tannins and alkaloids.[28, 29, 30] For years, the indigenous communities and traditional healers use its leaves as a very useful material to treat several diseases including intestinal disorders (Sandhya *et al*., 2010; Kane and Jawarkar 2017).[31, 32]).

However, despite these findings and traditional usage to treat intestinal disease and inflammation, no reports are available about the intestinal anti-inflammatory effects of *Glochidion ellipticum* Wight extract. Therefore, the present study has been designed to investigate the intestinal anti-inflammatory effects of this plant extract; through *in vitro* model of lipopolysaccharide (LPS) induced Raw 264.7 macrophage cells and *in vivo* colitis model using C57BL/6N mice in a dextran sulfate sodium (DSS) induced model after analyzing by ultra-high performance liquid chromatography/quadrupole time-of-flight mass spectrometry (UHPLC-Q-TOF-MS/MS).

Methods

Chemicals and reagents

DSS, sodium carboxymethyl cellulose (CMC-Na) and mesalazine were obtained from Shanghai Yuanye Bio-Technology Co., Ltd. (Shanghai, China). Fluorescein isothiocyanate labelled dextran (FITC-dextran, MW-4000) was purchased from Xi'an Ruixi Biological Technology Co., Ltd (Xi'an, China). Hemoccult kits were bought from Nanjing Jiancheng Bioengineering Institute (Nanjing, China). MTT assay kit, Bicinchoninic (BCA) protein assay kit, total nitric oxide (NO) assay kit, catalase (CAT) assay kit, myeloperoxidase (MPO) assay kit, superoxide dismutase (SOD) assay kit and malondialdehyde (MDA) assay kit were obtained from Beyotime Institute of Biotechnology, Ltd (Shanghai, China). RNA extraction kit was purchased from Transgen Biotech Co. Ltd (Beijing, China). LPS and DCFH-DA were brought from Sigma-Aldrich (St. Louis, MO, USA). Sodium pyruvate was purchased from Solarbio Life Sciences (Beijing, China). High-sig ECL Western Blotting Substrate was obtained from Tanon (Tanon, Shanghai, China). All other chemicals used in this study were of analytical grade and purchased from Beijing Chemical Works (Beijing, China).

Preparation of *G. ellipticum* extracts

Glochidion ellipticum Wight (Phyllanthaceae) as authenticated by Professor Shaikh Bokhtear Uddin, Department of Botany, Chittagong University, Chittagong, Bangladesh). Leaves were collected from Bandarban district, Bangladesh in February 2018. A voucher specimen was deposited in the herbarium of the Botany Department (CUBH-28941). Extracts were prepared following the methods described by Suradej *et al*.[33] After air drying at room temperature, 7.5 kg leaves were powdered in an industrial-grade grinder at low temperature and sieved using 315 µm sieve. Subsequently, the powder was placed in an automated sonicator assisted extractor (1:9, w/v) with different concentrations of ethanol from 100 to 70% (v/v) for extraction. Later, the extracts were further fractionated thrice by liquid–liquid extraction using hexane, dichloromethane and butanol to achieve three fractions, viz. hexane extract (HexE), dichloromethane extract (DcmE), butanol extract (ButE). The separations were concentrated by a rotary evaporator (Büchi Rotavapor R 3, BÜCHI Labortechnik AG, Switzerland) and dried by freeze dryer (Christ alpha 1–2/ LD plus, Germany) and stored at −20°C until used.

UHPLC-Q-TOF-MS/MS analysis of *G. ellipticum* extracts

5.0 mg freeze-dried sample from each type was dissolved in 1.0 ml 95% (v/v) ethanol. Then they were passed through a 0.22 µm nylon membrane filter before proceeding to UHPLC-Q-TOF/MS analysis. UHPLC-Q-TOF-MS/MS analysis was performed following the method described by Ma *et al*.,[34] with minor modification.

UHPLC analysis was performed on an Agilent 1290 UHPLC system (Agilent, Palo Alto, CA, USA) equipped with an Agilent ZORBAX Eclipse Plus C_{18} column (2.1 × 100 mm, 1.8 µm) at 40°C. The mobile phase consisted of a linear gradient of 0.1% (v/v) aqueous formic acid (A) and 0.1% (v/v) acetonitrile (B): 0–2.0 min, 5% B (v/v); 2.0–20.0 min, 5–100% B (v/v); 20.0–25.0 min, 100% B (v/v). The flow rate was 0.3 ml/min, and the injected volume was 2 µl. The column was reconditioned for 5 min prior to the next injection.

The MS analysis was performed on an Agilent 6545 Accurate-Mass Q-TOF/MS system equipped with an electrospray ionization (ESI) source connected to UHPLC. The ESI source parameters were: drying gas (N_2); flow rate and temperature, 10.0 l/min and 325°C; nebulizer, 35 psi; capillary voltages were 1500 and 3000 V in negative and positive modes, respectively. The mass screening range was *m/z* 100–1700. All data were recorded and processed using the Agilent MassHunter Workstation software (Version B.07.00), Agilent MSC software (Version B.07.00) and the Chinese medicine database (TCM library). The accuracy error threshold was set at ≤5 ppm.

Cell culture

Raw 264.7 macrophage cells were collected from Stem Cell Bank, Institute of Zoology (China Academy of Sciences, Beijing) and

maintained in Dulbecco's Modified Eagle Medium (DMEM) supplemented with 10% FBS, 1% glutamax and 1% sodium pyruvate at 37°C in 5% CO_2 atmosphere.

Cell viability assay

Cell viability was measured following the method followed by Ma *et al.*[35] Macrophage cells were seeded at 2 × 10^4 cells per well and incubated. After confirmation of confluency, the media was replaced with serum-free media with different doses of HexE, DcmE and ButE. Twenty-four hours later, media was changed and 20 µl MTT (5 mg/ml) added per well and incubated for four hours at 37°C and 5% CO_2. Formazan crystals formed in this step were dissolved by adding 10% SDS and incubated for 12 h. The absorbance was measured at 570 nm on a microplate reader (Tecan, Männedorf, Switzerland).

$$\% \text{ Cell viability} = \frac{\text{Absorbance of sample}}{\text{Absorbance of control}} \times 100$$

Determination of nitrite and intracellular reactive oxygen species scavenging activity in Raw 264.7 macrophage cells

Intercellular nitrite and ROS scavenging activity were measured following the methods by Lee *et al.*[36] Cells were seeded at 2 × 10^4 cells per well and incubated. After they reach confluency, serum-free media with LPS and different doses of HexE, DcmE and ButE replaced the media. Twenty-four hours after treatment, 60 µl supernatants were taken and added with Griess reagent as per kits instruction. After incubation at room temperature for 10 min, absorbance was measured at 540 nm on a microplate reader (Tecan, Männedorf, Switzerland).

For ROS measurement, 2 × 10^4 cells per well were seeded and incubated until they reach confluency. After that, serum-free media with LPS and different doses of HexE, DcmE and ButE used to replace the media. Then the media were replaced by DCFH-DA (10 µmol/ml) and incubated for 30 min at 37°C and 5% CO_2. Then, the media were thrown and wells were washed twice with PBS. Followed by wash, the wells were added serum-free media and fluorescence intensity was measured with an excitation wavelength of 485 nm and an emission wavelength of 535 nm using a spectrophotometer (Tecan, Männedorf, Switzerland).

Table 1 DAI scoring table (as per Sánchez-Fidalgo *et al.*[38])

Score	Weight loss (% of initial weight)	Stool consistency	Hemoccult test
0	<1%	Normal	Normal
1	1–4.99%	Slightly loose	Slightly bloody
2	5–9.99%	Very loose	Bloody
3	>10%	Diarrhea	Gross bleeding

Animal experimental design

Six-week-old female C57BL/6N mice were purchased from Beijing Vital River Laboratory Animal Technology Co. Ltd (Beijing, China). The animals were housed in a standard condition (24 ± 1°C with 50% humidity) and 12 h light/12 h dark cycle maintained. The animals used in this study were handled according to the procedures of the Ethical Committee for Animal Experimentation of Beijing Laboratory Animal Research and the National Institutes of Health Guide for the care and use of Laboratory Animals (Permit number: Pony-2020-FL-34). All the animals were handled as humanely as possible.

Experimental colitis

After acclimatization for one week, mice were randomly divided into six groups (n = 8). Colitis was induced by administrating 3% (w/v) DSS (MW: 50000) in drinking water ad libitum for 7 days, and the control group received only tap water.[37] After colitis induction, all groups were provided tap water for the following procedure. Then control and DSS group received only water, and the other four groups received different treatments by oral gavage for a week. Group three received 200 mg/kg HexE, dissolved in 0.5% CMC-Na; group four received 200 mg/kg DcmE, dissolved in 0.5% CMC-Na; group five received 200 mg/kg ButE, dissolved in 0.5% CMC-Na; and group six (standard drug group) were given 100 mg/kg mesalazine, dissolved in 0.5% CMC-Na. Bodyweight change, stool consistency and stool blood status were recorded every day to calculate the disease activity index (DAI) score for each mouse. The analyzing criteria for DAI calculation are shown in Table 1. The DAI was calculated according to a previously reported method of Sánchez-Fidalgo *et al.*[38]

Histopathological analysis of dextran sulfate sodium-induced colon tissues

Distal colon samples were taken for histology analysis as per the method followed by Mehmood *et al.*[39] Shortly after dissection, colon samples were collected, cleaned properly with ice-cold PBS and then distal colon samples were fixed in 10% buffered formalin for a day. After that, formalin-fixed samples were embedded in paraffin and later cut into 5 mm sections. After that, those sections were stained with hematoxylin and eosin. Finally, they were observed under a microscope for histological damage analysis. The histological damage scoring parameters and scoring system are presented in Table 2. The Caseviewer version 2.1 was used to analyze each picture.

In vivo permeability assay

To determine the barrier integrity of mice, *in vivo* permeability assay was performed using FITC-dextran as described previously.[40] On the day of sacrifice, FITC-dextran dissolved in water was given to

Table 2 Histopathological scoring system

Tissue damage		Extent of damage		Crypt damage		Inflammation	
Parameter	Score	Parameter	Score	Parameter	Score	Parameter	Score
No damage	0	Only in mucosa	1	Basal 1/3 damage	1	Minor	1
<25%	1	Mucosa and submucosa	2	Basal 2/3 damage	2	Moderate	2
26–50%	2	Beyond submucosa	3	Up to epithelium	3	Severe	3
51–75%	3			Crypt and epithelium lost	4		
76–100%	4						

each mouse at 600 mg/kg dose after depriving them of food and water. Four hours after FITC-dextran administration, mice were euthanized and sacrificed. Afterwards, blood was collected via cardiac puncture, centrifuged at 2000 × *g* for 15 min at 4°C and supernatants were separated in a new Eppendorf tube. Later, fluorescence intensity was measured at 492 nm excitation and 525 nm emission using a spectrophotometer (Tecan, Männedorf, Switzerland).

Nitric oxide, malondialdehyde, catalase , superoxide dismutase and myeloperoxidase measurement

As DSS treatment causes a significant change in liver functions and metabolism, liver samples were also taken into consideration for analysis.[41] Abnormally high gut permeability results in the influx of LPS, flagellin and other antigens into the liver through the renal portal vein. These antigens cause a high-level immune response and oxidative stress in the liver, and hence liver is a crucial part to investigate the abnormalities.[42] Briefly, colonic and liver tissue samples were washed with PBS to clear off any waste materials. Subsequently homogenized with PBS, and then centrifuged at 3000 *g* for 10 min at 4°C. After that, the supernatants were collected in another clean Eppendorf tube and each assay was performed following the manufacturer's instructions. Griess method was used to determine live NO content.[43] MDA level was determined following the procedure of Zhang *et al*.,[44] CAT and SOD activity were measured following the methods described by Chen *et al*.[45] Colonic MPO activity was measured by following the method used by Cho *et al*.[46]

Real-time PCR

Total RNA from cells was extracted using Trizol reagent (Transgen biotech, Beijing, China) following the manufacturer's instructions. Later, the concentration was measured at 260/280 ratio using a spectrophotometer (Tecan, Männedorf. Switzerland). The RNA was then reverse-transcribed using ReverTra Ace qPCR RT master mix with gDNA remover (Toyobo, Japan). 0.5 µg RNA from macrophage cells were used for RT-PCR. The mRNA expression levels of the following genes were quantified following:[47] TNF-α; interleukin-1β (IL-1β); IL-6 and β-actin. β-actin was used as a positive control. RT-PCR was performed with a BioRad CFX96 touch system using the SYBR Green master mix (Toyobo, Japan). The sequences of primers used are given in Table 3.

Western blot analysis

Collected colon samples and macrophage cells were washed in ice-cold PBS, homogenized in ice-cold lysis buffer containing protease inhibitor and phosphatase inhibitor as per kits instruction (Nanjing Jiancheng Bioengineering Institute, Nanjing, China). Then, the homogenates were kept in ice for 30 min and later centrifuged at 1008 × *g* for 15 min at 4°C. The supernatants were separated and protein concentrations were quantified by using BCA protein assay following the microplate procedure. 30 µg proteins from each sample were separated by sodium dodecyl sulfate-polyacrylamide gel electrophoresis (SDS-PAGE) and then transferred to polyvinylidene difluoride membrane (Merck KGaA, Darmstadt, Germany). The membrane was blocked at 4°C with 5% non-fat milk in tris-buffer saline (TBST). The membrane was then incubated with primary antibodies (mice anti-β-actin, rabbit anti-iNOS, then washed with TBST thrice. After that, the membrane incubated with secondary antibodies for 2 h at room temperature. Finally, Tanon High-sig ECL Western Blotting Substrate (Tanon, Shanghai, China) was applied to the membrane to visualize the band density as per manufactures instruction. Finally, using ImageJ image processing software (ImageJ, National Institutes of Health, Bethesda, MD, USA), bands were quantified as per their density and evaluated.

Table 3 Primer sequence used for RT-PCR

Name	Primer	Sequence
β-Actin	Forward	5′-CCTCTATGCCAACACAGT-3′
	Reverse	5′-AGCCACCAATCCACACAG-3′
IL-6	Forward	5′-AGTAAGTTCCTCTCTTGCAAGAGACT-3′
	Reverse	5′-CACTAGGTTTGCCGAGTAGATCTC-3′
TNF-α	Forward	5′-ATGAGCACAGAAAGCATGATCCGC-3′
	Reverse	5′-CCAAAGTAGACCTGCCCGGACTC-3′
IL-1β	Forward	5′-ATGGCAATCGTTCCTGAACTCAAC-3′
	Reverse	5′-CAGGACAGGTATAGATTCTTTCCTTT-3′

Statistical analysis

All experiments were carried out in triplicate. Results are expressed as mean ± standard deviation (SD). Comparisons were executed using the one-way analysis of variance (ANOVA) test using GraphPad Prism (version 8.0.2; GraphPad Software Inc., San Diego, CA, USA). Below 0.05 *P* values were considered statistically significant.

Results

UHPLC-Q-TOF-MS/MS Analysis

All the compounds were detected in negative mode from the total ion chromatogram (TIC) with the aid of Agilent MassHunter Workstation and by comparing with the reference standard compounds. As shown in Table 4a, 11 compounds were tentatively identified form the HexE, mostly phenolic compounds and terpenes. Among them, the most significant are eupatilin (peak 8), α-linolenic acid (peak 10) and oleanolic acid (peak 11) (Figure 1). Table 4b shows the components of DcmE, the majority of which are phenolic compounds. Gallic acid (peak 1), epicatechin (peak 5) and syringic acid (peak 8) are the key compounds present in this fraction (Figure 2). Table 4c contains the analysis of ButE, of which most are terpenoids and phenolics. Among them, vital ones are monotropein (peak 1), gallocatechol (peak 4) and epigallocatechin (peak 6) (Figure 3).

In vitro analysis

Effects of hexane extract, dichloromethane extract and butanol extract on cell viability

MTT assay was performed to determine the cytotoxicity of the different doses of HexE, DcmE and ButE. All three extracts up to 100 µg/ml maintained the stability of the cells, i.e. more than 90% viable. Higher than 100 µg/ml dose has a deleterious effect on the cells (Figure 4) and hence for the next experiments, nontoxic doses were used to rule out the possibility of *G. ellipticum* extracts effects due to cell viability reduction.

Effects of hexane extract, dichloromethane extract and butanol extract on nitric oxide production

As a counter effect of LPS treatment, cells secret nitric oxide, which is involved in numerous inflammatory processes. The iNOS, eNOS and nNOS are the regulators of NO production, but the latter two of them are calcium-dependent. Only, iNOS is triggered by extracellular stimuli like cytokines and chemokines. For HexE,

Table 4 Composition of HexE, DcmE and ButE

Peak	Compound	Formula	RT	Observed mass $[M-H]^-$	Reference mass $[M-H]^-$	CAS ID
(a) Composition of HexE						
1	Quinic acid	$C_7H_{12}O_6$	1.04	192.0637	192.0634	77-95-2
2	Ellagic acid	$C_{14}H_6O_8$	6.619	302.0073	302.0063	476-66-4
3	Thymol	$C_{10}H_{14}O$	7.549	150.1057	150.1045	89-83-8
4	Taxifolin	$C_{15}H_{12}O_7$	8.274	304.0594	304.0583	480-18-2
5	Rhapontigenin	$C_{15}H_{14}O_4$	8.503	258.0901	258.0892	500-65-2
6	Linalool	$C_{10}H_{18}O$	10.089	154.1366	154.1358	78-70-6
7	Sclareolide	$C_{16}H_{26}O_2$	12.711	250.1955	250.1933	564-20-5
8	Eupatilin	$C_{18}H_{16}O_7$	14.153	344.0917	344.0896	22368-21-4
9	Corylin	$C_{20}H_{16}O_4$	15.57	320.1071	320.1049	53947-92-5
10	α-Linolenic acid	$C_{18}H_{30}O_2$	17.134	278.2263	278.2246	463-40-1
11	Oleanolic acid	$C_{30}H_{48}O_3$	18.579	456.3634	456.3604	508-02-1
(b) Composition of DcmE						
1	Gallic acid	$C_7H_6O_5$	1.49	170.0223	170.0215	149-91-7
2	Methyl gallate	$C_8H_8O_5$	2.693	184.0382	184.0372	99-24-1
3	4-Carboxyphenol	$C_7H_6O_3$	4.405	138.0324	138.0317	99-67-7
4	2,6-Dimethoxyphenol	$C_8H_{10}O_3$	4.965	154.0638	154.063	91-10-1
5	Epicatechin	$C_{15}H_{14}O_6$	5.381	290.0806	290.079	490-46-0
6	Benzoic acid	$C_7H_6O_2$	5.647	122.0372	122.0368	65-85-0
7	Gallocatechin gallate	$C_{22}H_{18}O_{11}$	6.252	458.0874	458.0849	4233-96-9
8	Syringic acid	$C_9H_{10}O_5$	6.779	198.0538	198.0528	530-57-4
9	Propyl gallate	$C_{10}H_{12}O_5$	8.265	212.0695	212.0685	121-79-9
10	Alkannin	$C_{16}H_{16}O_5$	9.008	288.1014	288.0998	517-88-4
11	Myristic acid	$C_{14}H_{28}O_2$	10.355	228.2101	228.2089	544-63-8
12	Parthenolide	$C_{15}H_{20}O_3$	11.719	248.1422	248.1412	20554-84-1
13	Isomoreollic acid	$C_{34}H_{40}O_9$	19.848	592.2697	592.2672	1240792-57-7
(c) Composition of ButE						
1	Monotropein	$C_{16}H_{22}O_{11}$	1.652	390.116	390.1162	5945-50-6
2	8-O-Acetylharpagide	$C_{17}H_{26}O_{11}$	2.785	406.147	406.1475	6926-14-3
3	Eugenol	$C_{10}H_{12}O_2$	4.861	164.084	164.0837	97-53-0
4	Gallocatechol	$C_{15}H_{14}O_7$	5.076	306.0747	306.074	970-73-0
5	Mulberrin	$C_{25}H_{26}O_6$	6.047	422.173	422.1719	62949-79-5
6	Epigallocatechin	$C_{15}H_{14}O_7$	7.082	306.0744	306.074	970-74-1
7	Arbutin	$C_{12}H_{16}O_7$	9.377	272.0875	272.0896	497-76-7

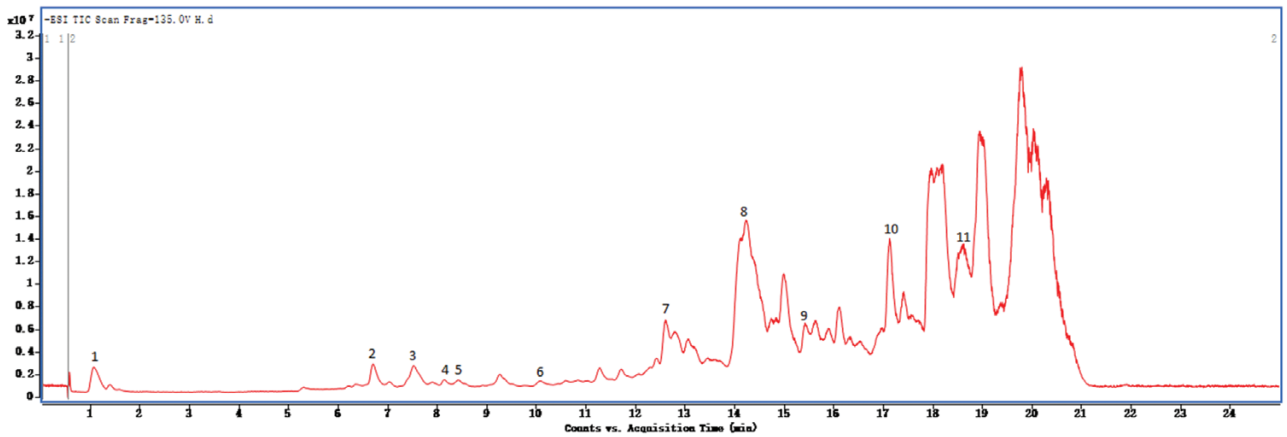

Figure 1 Total ion chromatogram obtained by UHPLC-Q-TOF/MS of hexane extract (HexE).

compared to control group, LPS treatment increased the nitrite level by 821.798% ($P < 0.01$). Treatments with 5, 10, 20, 25, 50 and 100 μg/ml HexE reduced the nitrite level by 31.26%, 46.29%, 51.41%, 65.12%, 68.49% and 84.94% compared to LPS group ($P < 0.001$) (Figure 5a). As for DcmE, nitrite level increased by 662.23% in LPS group compared to control group ($P < 0.0001$). 5, 10, 20, 25, 50 and 100 μg/ml treatment doses decreased the nitrite level by 19.81%, 30.07%, 49.32%, 79.48%, 84.83% and 96.34% ($P < 0.0001$) (Figure 5b). Nitrite level increased by 1232.86% ($P < 0.01$) in the LPS group compared to normal control for ButE. Treatments with 5, 10, 20, 25, 50 and 100 μg/ml ButE lowered the nitrite level by 5.38%, 13.98%, 30.26%, 41.24%, 66.59% and 92.17% ($P <$

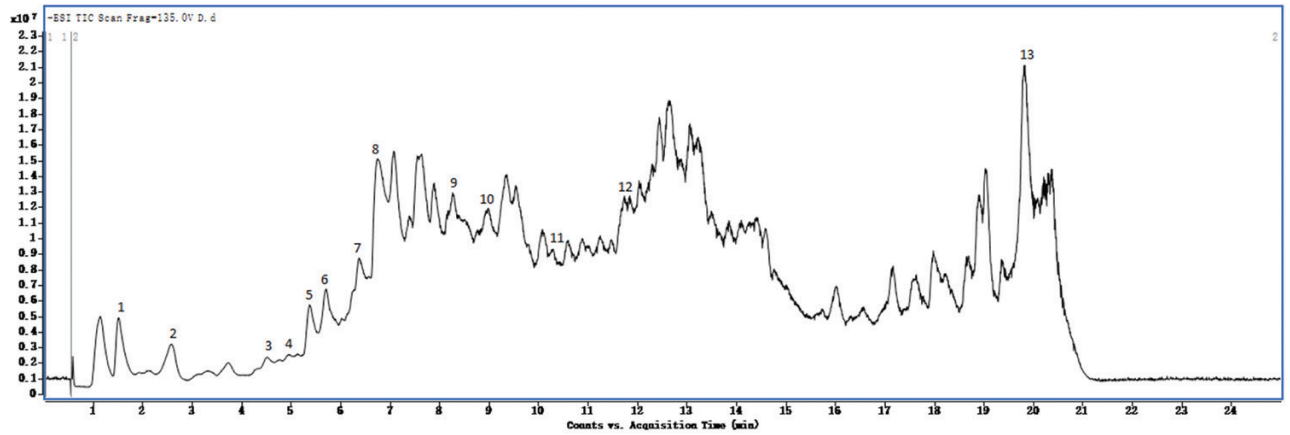

Figure 2 Total ion chromatogram obtained by UHPLC-Q-TOF/MS of dichloromethane extract (DcmE).

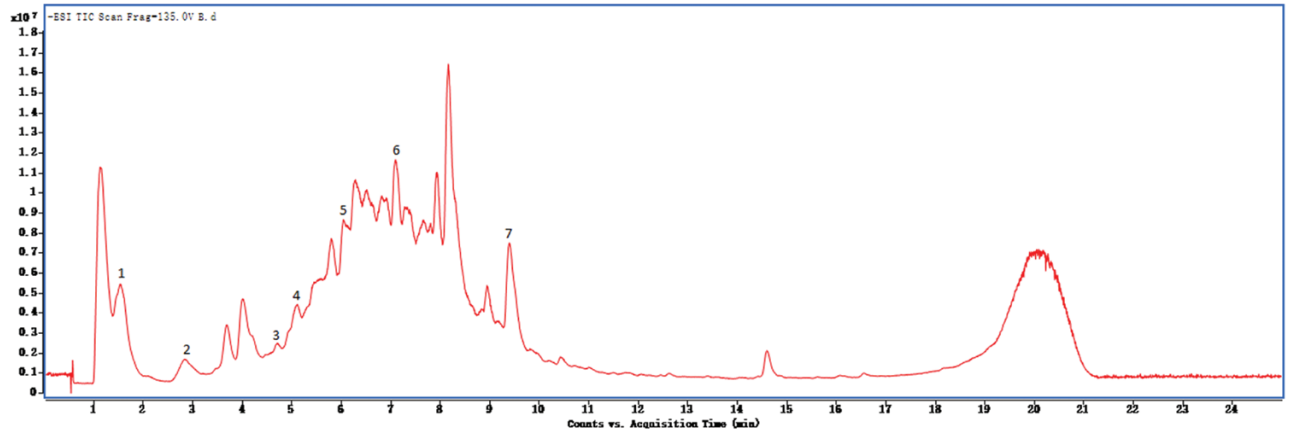

Figure 3 Total ion chromatogram obtained by UHPLC-Q-TOF/MS of butanol extract (ButE).

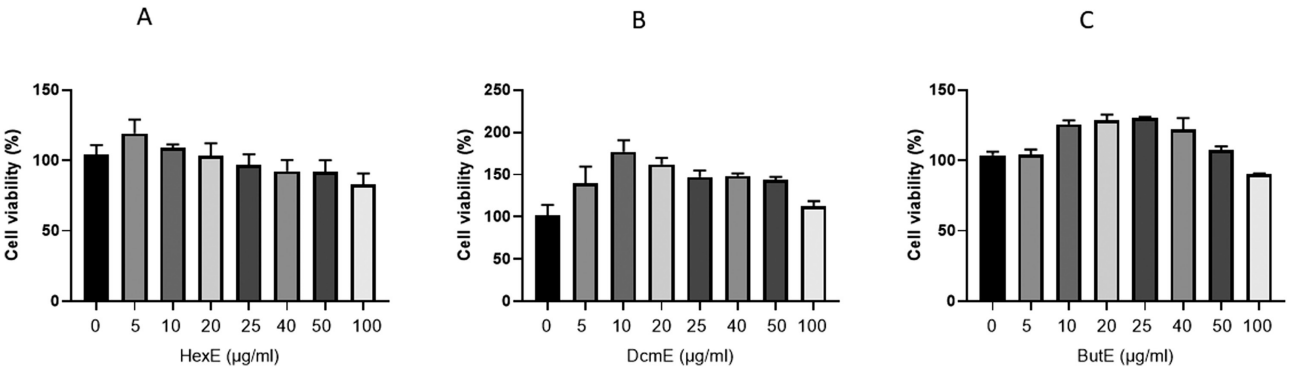

Figure 4 The MTT assay performed with RAW 264.7 macrophage cells. Murine macrophage cell line (2 × 10^4 cells/well) was incubated for 24 h with different concentrations of hexane extract (HexE) (A), dichloromethane extract (DcmE) (B) and butanol extract (ButE) (C) (5–100 µg/ml). Each data point represents the mean ± SD (n = 3).

0.001) (Figure 5c). Fluctuation in cellular NO level, directly affects ROS production.[48]

Effect of hexane extract, dichloromethane extract and butanol extract on cellular reactive oxygen species production

ROS production increased by 111.98% ($P < 0.01$) in the LPS group compared to control group for HexE. 5, 10, 20, 25, 50 and 100 µg/ml HexE reduced the ROS level by 32%, 38.88%, 53.08%, 57.58%, 74.35% and 77.85% compared to LPS group ($P < 0.001$) (Figure 6a). In case of DcmE, ROS level increased 151.65% ($P < 0.01$) in the LPS group respect to the control group. DcmE treatments of 5, 10, 20, 25, 50 and 100 µg/ml diminished the ROS level by 16.75%, 23.04%, 35.66%, 47.85%, 84.48% and 91.56% against LPS group ($P < 0.0001$) (Figure 6b). For ButE, ROS level

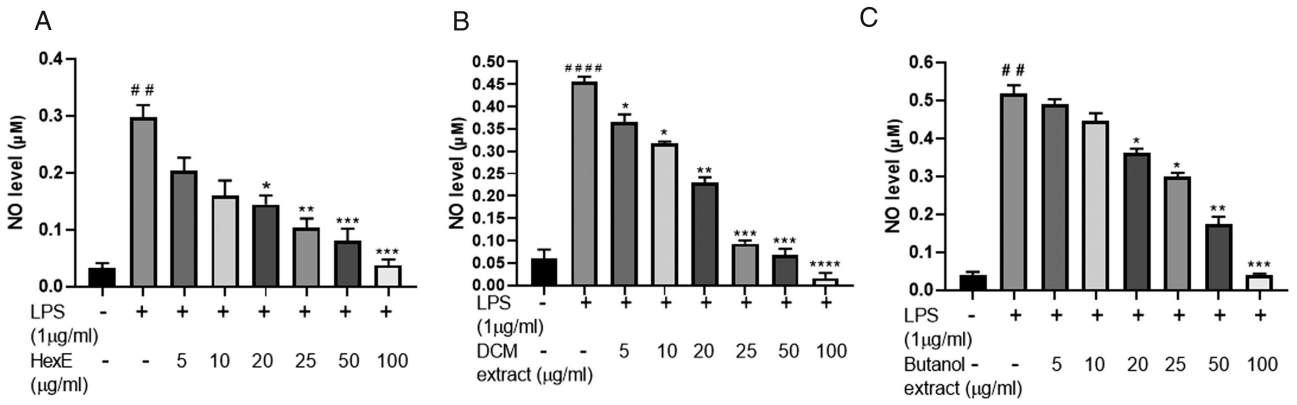

Figure 5 Effect on nitric oxide production by Lipopolysaccharide (LPS) induced RAW 264.7 macrophage cells. 2 × 10^4 cells/well was incubated for 24 h with different concentrations of hexane extract (HexE) (A), dichloromethane extract (DcmE) (B) and butanol extract (ButE) (C) (5–100 μg/ml) and lipopolysaccharide (LPS) (1 μg/ml) . Each data point represents the mean ± SD ($n = 3$). ##$P < 0.01$ versus control group; *$P < 0.05$ versus LPS group, **$P < 0.01$ versus LPS group, ***$P < 0.001$ versus LPS group, ****$P < 0.0001$ versus LPS group.

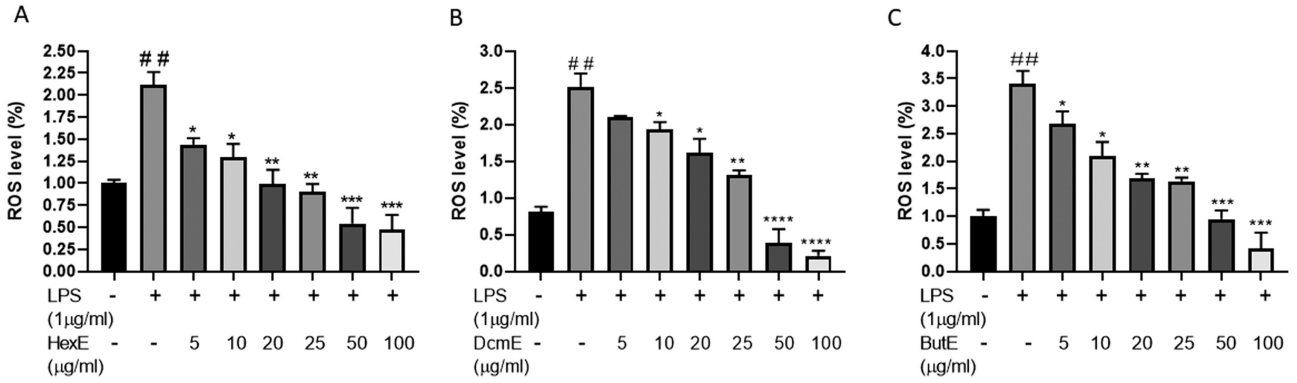

Figure 6 Effect of *Glochidion ellipticum* extracts on lipopolysaccharide (LPS) induced cellular reactive oxygen species (ROS) production. 2 × 10^4 cells/well was incubated for 24 h with different concentrations of hexane extract (HexE) (A), dichloromethane extract (DcmE) (B) and butanol extract (ButE) (C) (5–100 μg/ml) and LPS (1 μg/ml). Each data point represents the mean ± SD ($n = 3$). ##$P < 0.01$ versus control group; *$P < 0.05$ versus LPS group, **$P < 0.01$ versus LPS group, ***$P < 0.001$ versus LPS group, ****$P < 0.0001$ versus LPS group.

climbed by 240.264% ($P < 0.01$) in LPS group against control group. ButE treatments of 5, 10, 20, 25, 50 and 100 μg/ml lowered the ROS level by 38.43%, 43.08%, 52.42%, 61.43%, 88.52% and 93.76% as compared to LPS group ($P < 0.001$) (Figure 6c). ROS is directly associated with inflammation and proinflammatory cytokine regulation.[49]

Hexane extract, dichloromethane extract and butanol extract inhibited pro-inflammatory cytokines expression

To assess the effects of *G. ellipticum* extracts, we analyzed the mRNA expression of iNOS, TNF-α, IL-6 and β-actin on macrophage cells. LPS treatment increased the TNF-α level by 273.72% compared to normal control ($P < 0.01$) (Figure 7a). 5, 10 and 20 μg/ml dose of HexE reduced the increased TNF-α level by 60.76%, 78% and 90.4%, respectively ($P < 0.01$). Figure 7b depicts the analysis of DcmE. LPS treatment increases the TNF-α level by 1211.53% ($P < 0.001$). DcmE at the dose of 5, 10 and 20 μg/ml lowered the increased level by 20.55%, 40.11% and 64.17% ($P < 0.01$). The result of ButE is shown in Figure 7c. Compared to normal control, LPS increased TNF-α by 1241.9% ($P < 0.01$). 5, 10 and 20 μg/ml of ButE lessened the elevated level by 22.04%, 58.49% and 81.44% ($P < 0.0001$).

Figure 8 includes the results for *G. ellipticum* extracts on LPS stimulated macrophage cells. LPS elevated the IL-1β expression compared to normal control by 398.9% ($P < 0.001$) (Figure 8a). HexE of 5, 10 and 20 μg/ml lowered the increased level by 19.71%, 54.87% and 75.17% ($P < 0.001$). IL-1β expression increased by 255.57% in LPS group compared to normal control ($P < 0.01$) (Figure 8b). 5, 10 and 20 μg/ml DcmE lessened the IL-1β expression by 75.04%, 89.41 and 94.80% ($P < 0.01$). Compared to control group, 363.33% increase of IL-1β is seen in LPS group ($P < 0.001$) (Figure 8c). ButE at 5, 10 and 20 μg/ml dose reduced the expression by 13.67%, 43.89% and 57.91%, respectively ($P < 0.01$).

Figure 9 presents the outcome of LPS and *G. ellipticum* extracts on macrophage cells. LPS increased iNOS expression by 263.35% compared to normal control ($P < 0.001$). HexE at the dose of 5, 10 and 20 μg/ml lessened the elevated expression by 73.93%, 87.38% and 97.56% ($P < 0.001$) (Figure 9a). iNOS expression increased by 252.44% in LPS induced macrophage cells ($P < 0.01$). 5, 10 and 20 μg/ml DcmE lowered iNOS expression by 33.73%, 48.07% and 95.72% ($P < 0.01$) (Figure 9b). LPS elevated iNOS expression by 320% ($P < 0.001$). ButE at the dose of 5, 10 and 20 μg/ml dropped the elevated expression by 15.95%, 30.96% and 59.13%, respectively ($P < 0.01$) (Figure 9c).

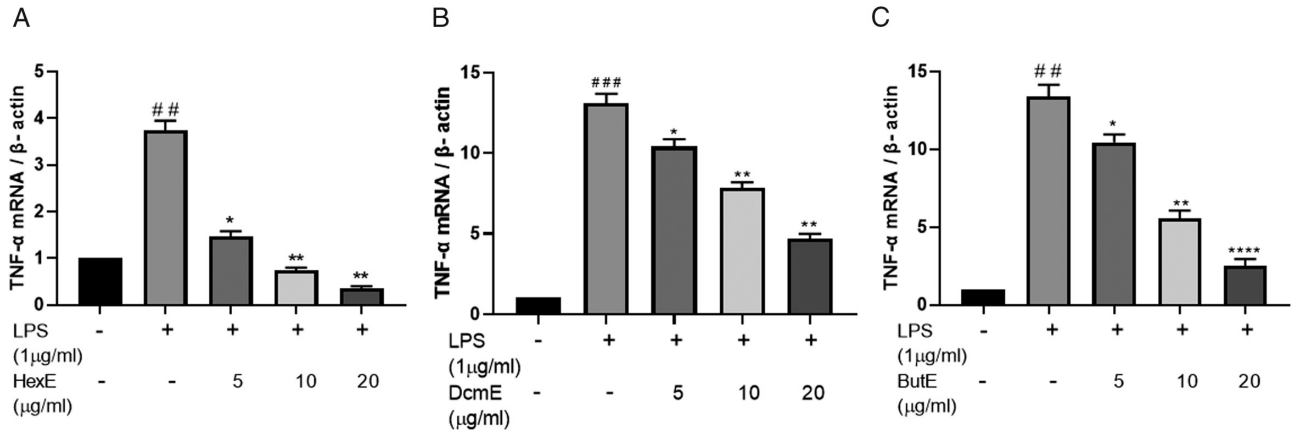

Figure 7 Hexane extract (HexE) (a), dichloromethane extract (DcmE) (b) and butanol extract (ButE) (c) reduce TNF-α expression. Data are represented as the mean ± SD ($n = 3$). ##$P < 0.01$ versus control group, ###$P < 0.001$ versus control group; *$P < 0.05$ versus LPS group, **$P < 0.01$ versus LPS group, ****$P < 0.0001$ versus LPS group.

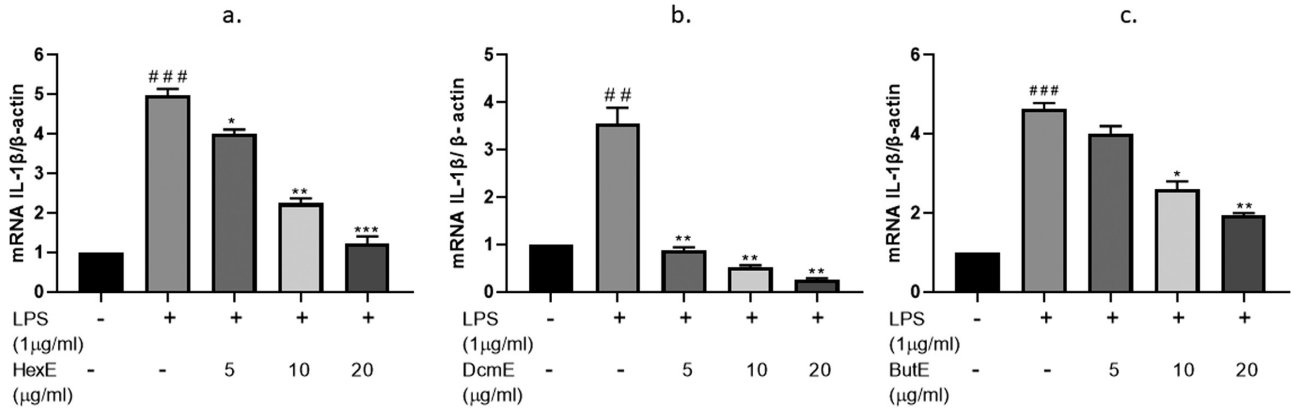

Figure 8 Hexane extract (HexE) (a), dichloromethane extract (DcmE) (b) and butanol extract (ButE) (c) reduce IL-1β expression. Data are represented as the mean ± SD ($n = 3$). ##$P < 0.01$ versus control group, ###$P < 0.001$ versus control group; *$P < 0.05$ versus LPS group, **$P < 0.01$ versus LPS group, ***$P < 0.001$ versus LPS group.

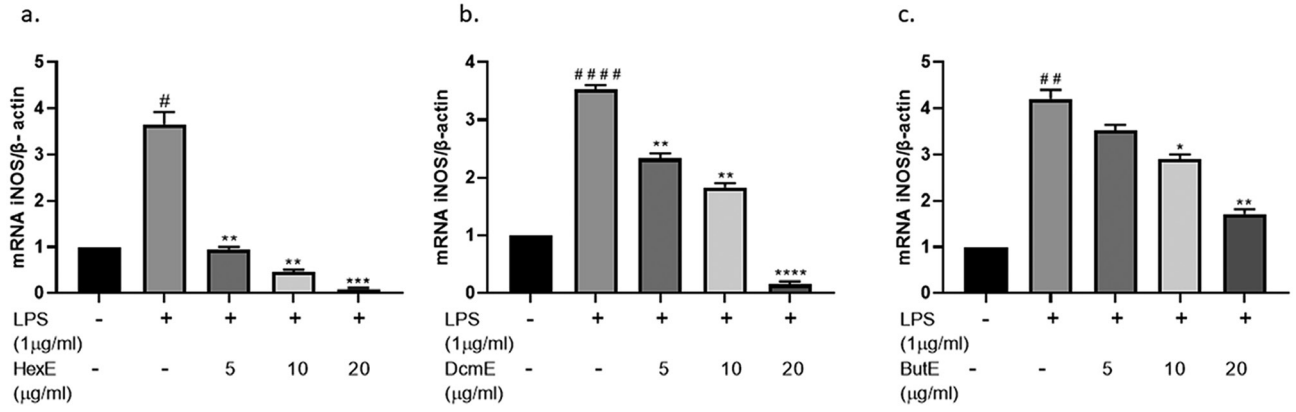

Figure 9 Hexane extract (HexE) (a), dichloromethane extract (DcmE) (b) and butanol extract (ButE) (c) reduce Inducible nitric oxide synthase (iNOS) expression. Data are represented as the mean ± SD ($n = 3$). #$P < 0.05$ versus control group, ##$P < 0.01$ versus control group, ####$P < 0.0001$ versus control group; *$P < 0.05$ versus LPS group, **$P < 0.01$ versus LPS group, ***$P < 0.001$ versus LPS group.

In vivo analysis

Effect of *Glochidion ellipticum* extracts on disease activity index score

The main visible clinical feature of DSS induced acute colitis is bloody stool along with weight loss. DSS group exhibited a marked increase of DAI score on day 5 and reached maximum on the day 11 compared to the initial score ($P < 0.01$). Oral administration of three *G. ellipticum* extracts reduced DAI score compared to the DSS group and statistically significant was HexE and ButE ($P < 0.05$) (Figure 10). Thus, *G. ellipticum* extracts attenuate pathological

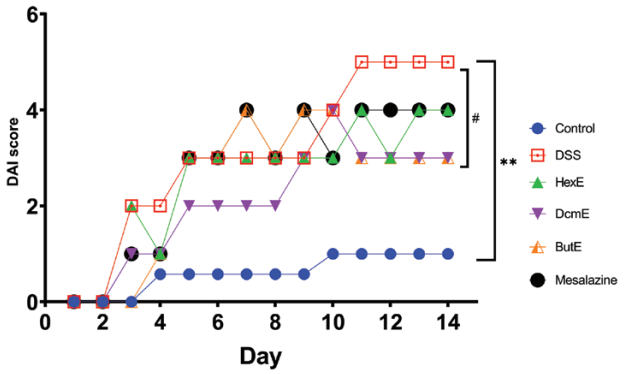

Figure 10 Assessment of DAI daily for each animal [DAI = (combined score of weight loss, stool consistency and stool blood). Data represented as the mean ± SD (n = 6). #P < 0.05 versus control group; **P < 0.01 versus DSS group.

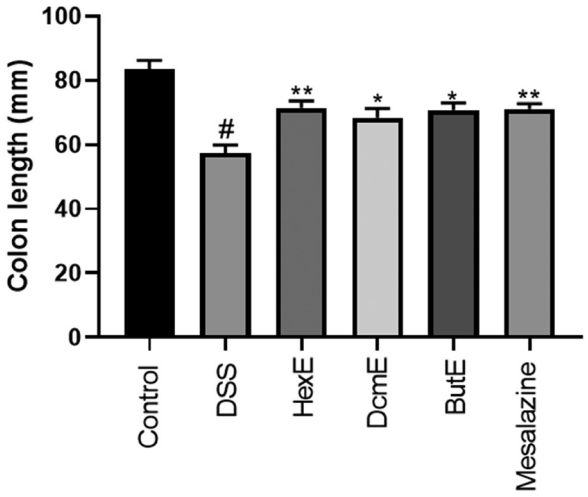

Figure 11 Colon length measurement results showing the protective role of hexane extract (HexE), dichloromethane extract (DcmE) and butanol extract (ButE) against dextran sulfate sodium (DSS) induced colonic damage. Data represented as the mean ± SD (n = 6). #P < 0.05 versus control group; *P < 0.05 versus DSS group, **P < 0.01 versus DSS group.

symptoms of acute colitis. Besides the DAI score, colon length is another parameter for DSS induced colitis. DSS significantly (P < *0.05*) reduced colon length which was restored by the *G. ellipticum* extracts and HexE was most significant (P < *0.01*) among all three extracts and the significance level was the same as standard drug group (Figure 11).

Glochidion ellipticum extracts restore histopathological damage

Light microscopy of H&E stained colonic slides of the DSS group showed typical tissue damage, ulceration, crypt damage and inflammation as indicated by the presence of neutrophils in the epithelium and the adjacent areas. As shown in Figure 12, DSS induction caused significant damage in the colon of the DSS group compared to the normal group (P < *0.0001*). On the other hand, oral administration of three *G. ellipticum* extracts (HexE, DcmE and ButE) restored intestinal damage caused by DSS administration and among them, ButE restored intestinal damage most (P < *0.0001*). The outcome of mesalazine treatment is also similar to *G. ellipticum* extracts, which indicates the colitic attenuating ability of these extracts.

Glochidion ellipticum extracts reduce increased permeability

Proper intestinal barrier function is a key feature to maintain a healthy gut and body as it blocks detrimental substances to enter the bloodstream and cause subsequent damages. Any damage to the barrier would end up in colitis and systematic inflammation. To determine the barrier integrity, we performed serum biochemical analysis with FITC-dextran. Compared to normal control, mice in the DSS group showed a 42.62% increase in serum level of FITC-dextran (P < *0.05*) (Figure 13). Administration of HexE, DcmE, ButE and Mesalazine lowered the serum FITC-dextran level by 42.32%, 18.06%, 25.5% and 41.38%. HexE and Mesalazine gave the best outcome and almost normalized the level to the control group (P < *0.01*).

Antioxidant effects on liver and colon

Damage to epithelial layer and increased permeability readily results in imbalance of antioxidant level. Activities of colonic and liver enzymes are shown in Figure 14. DSS significantly increased the activities of the liver MDA level by 90.01% compared to the control group (P < *0.05*) (Figure 14A). HexE, DcmE, ButE and Mesalazine reduced the increased level by 57.71% (P < *0.001*), 42.56% (P < *0.01*), 20.43% (P < *0.05*) and 63.49% (P < *0.001*). HexE group is almost the same as the standard drug group and the level is close to the control group itself. Liver NO level increased significantly by 185% in the DSS group compared to the control group (P < *0.01*) (Figure 14B). All three *G. ellipticum* extracts (HexE, DcmE and ButE) along with mesalazine reduced the increased level by 54.74%, 74.36%, 66.84% and 82.75% (P < *0.01*). Colonic MPO level increased quite significantly in the DSS group compared to the control group by 1250.9% (P < *0.0001*) (Figure 14C). Treatment with *G. ellipticum* extracts (HexE, DcmE and ButE) and Mesalazine lowered MPO level by 76.26%, 49.51%, 72.35% and 89.38%, respectively (P < *0.01*).

DSS treatment lowered the SOD level considerably (77.79%), compared to the normal group (P < *0.001*). *G. ellipticum* extracts (HexE, DcmE and ButE) elevated SOD level by 173.17%, 172.29% and 236.37% while mesalazine increased the SOD level by 243.7% (Figure 14D). ButE and Mesalazine restored the SOD level almost close to the normal control group (P < *0.05*). CAT activity was not influenced much by DSS, yet it reduced to some extent (Figure 14E). However, *G. ellipticum* extracts raised the CAT level significantly along with the standard drug group (P < *0.05*). Enzymatic imbalance and ROS overproduction activate COX-2and iNOS pathway, thereby causes severe inflammation and damage.[50]

Glochidion ellipticum inhibits dextran sulfate sodium induced inflammation by mediating cyclooxygenase-2 and inducible nitric oxide synthase pathway

NF-κB is a key mediator of inflammatory and immune responses. It controls the production of cytokines and mediates the expression of other downstream genes involved. Patients with IBD and colitic mice show increased expression of NF-κB. COX-2and iNOS are very popular downstream targets of NF-κB, which leads to inflammation and later complications including IBD. Immunoblotting was applied to estimate the level of COX-2 and iNOS on the colonic tissue. DSS treatment significantly increased the level of iNOS by 60.33% (P < *0.01*) in the colonic tissue compared to the control group. Treatment with *G. ellipticum* extracts (HexE, DcmE and ButE) and mesalazine lowered (P < *0.01*) the increased level of iNOS by 17.54%, 49.06%, 51.21% and 44.09% (P < *0.01*) (Figure 15A). DcmE and ButE gave

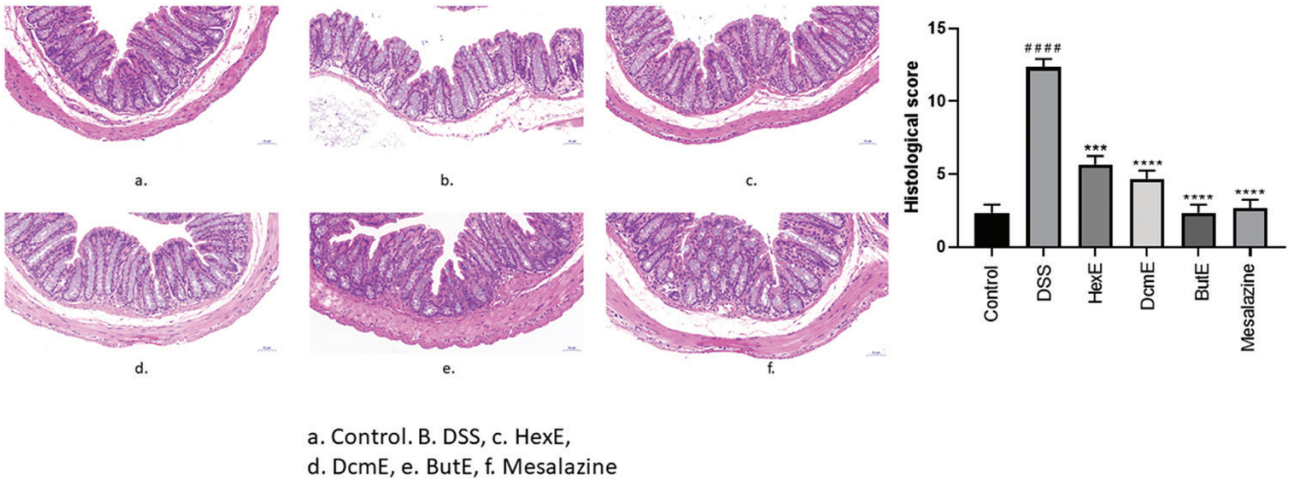

Figure 12 Hexane extract (HexE), dichloromethane extract (DcmE), butanol extract (ButE) attenuates dextran sulfate sodium (DSS)-induced colitis in C57BL/6 mice. Mice were treated with 3% DSS in their drinking water for 7 days to induce colitis. HexE, DcmE and ButE (200 mg/kg) was administered for 7 days after colitis induction. Mesalazine (100 mg/kg) was administered as standard drug. The colons from each experimental group were processed for histological evaluation (hematoxylin–eosin staining, 20×; scale bar, 50 μm). Data represented as the mean ± SD ($n = 6$). ####$P < 0.0001$ versus control group; ***$P < 0.001$ versus DSS group, ****$P < 0.0001$ versus DSS group.

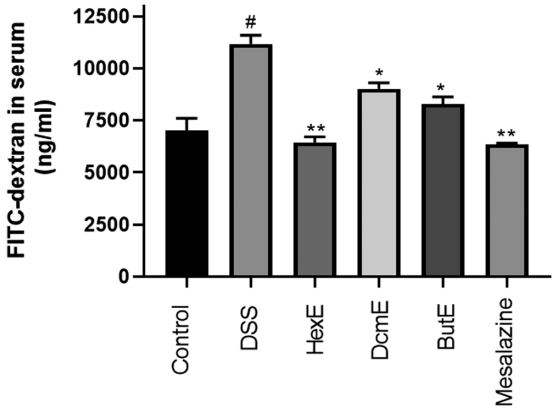

Figure 13 Levels of Fluorescein isothiocyanate–dextran (FITC-dextran) in the serum of dextran sulfate sodium (DSS) colitic and normal mice administered with FITC dextran were measured as an indicator of intestinal permeability. Data represented as the mean ± SD ($n = 6$). #$P < 0.05$ versus control group; *$P < 0.05$ versus DSS group, **$P < 0.01$ versus DSS group.

the best result and almost the same as the normal control group. Compared to normal mice, COX-2 expression was significantly higher in the DSS group ($P < 0.05$) (Figure 15B). The elevated expression of COX-2 was alleviated by HexE, DcmE, ButE and mesalazine by 48.26%, 37.37%, 71.11% and 20.67%; among these, ButE was very significant ($P < 0.001$).

Discussion and Conclusion

Natural products are in use to treat diseases and complications since the beginning of millennia. The increase of public interest to natural and safer products for everyday uses leading us to the way, which should always have chosen.[51] Synthetic drugs may provide a quick and easy remedy, but their actions are like double-edged sword. After sometimes of their use, our body and innate immune system become lethargic, and then the complications begun.[52] In this circumstance, we intended to evaluate a medicinal plant along with chemical components, which is being used by an ethnic community. UHPLC-Q-TOF/MS revealed the composition of *G. ellipticum* extracts which are mainly phenolic compounds and terpenoids. Eupatilin, α-linoleic acid, oleanolic acid, gallic acid, epicatechin, syringic acid, monotropein, gallocatechin and epigallocatechin are among the major compounds identified in the extracts. There is much evidence to support the antioxidative and anti-inflammatory properties of terpenoids and phenolics.[53, 54] Damages of colitis inducers like DSS, TNBS and acetic acid have been significantly restored mucosal injury by the treatment of polyphenols and terpenoids. The mechanism behind this recovery may be the reduction of and protection against oxidative stress, safeguarding of epithelial barrier function, lower immune cell responses and rectification of gut microbiota dysbiosis.[25, 55] Among the identified compounds four flavonoids were detected, viz. eupatilin, gallocatechol, epicatechin and epigallocatechin, that downregulates the activation of NF-κB upregulated by DSS.[56, 57, 58, 59] α-linoleic acid is another compound identified that normalizes TNBS induced colitis via the Th1/Th2/Th17 pathway.[60] In DSS induced colitis, oleanolic acid, another constituent of *G. ellipticum*, was capable of reducing inflammation by suppressing TNF-α, IL-6, IL-1β by restoring the balance of Th17/Treg cells and inhibiting NF-κB pathway.[61] Syringic acid and gallic acid are the phenolic acids present in *G. ellipticum* extract, alters experimental colitis by inhibiting the nuclear translocation and activation of p65-NF-κB and p-STAT-3^{Y705}.[62, 63] All these suggest that some of the polyphenolic compounds present in *G. ellipticum*, particularly the flavonoids, could be the reason behind the beneficial effects on DSS-induced experimental colitis.

To the best of our knowledge, this is the first time *G. ellipticum* extracts are being experimented in a DSS induced acute colitis model with C57BL/6N mice and LPS induced inflammation model on macrophage cells. In this study, we showed that *G. ellipticum* extracts attenuate colitis by reducing the DAI score, which was further confirmed by H & E staining score. Oral administration of DSS mimicked colitis in the mice, which were confirmed by several markers of IBD. Mice treated with *G. ellipticum* extracts significantly diminished those symptoms and restored the normal conditions which were almost close to the positive control group.

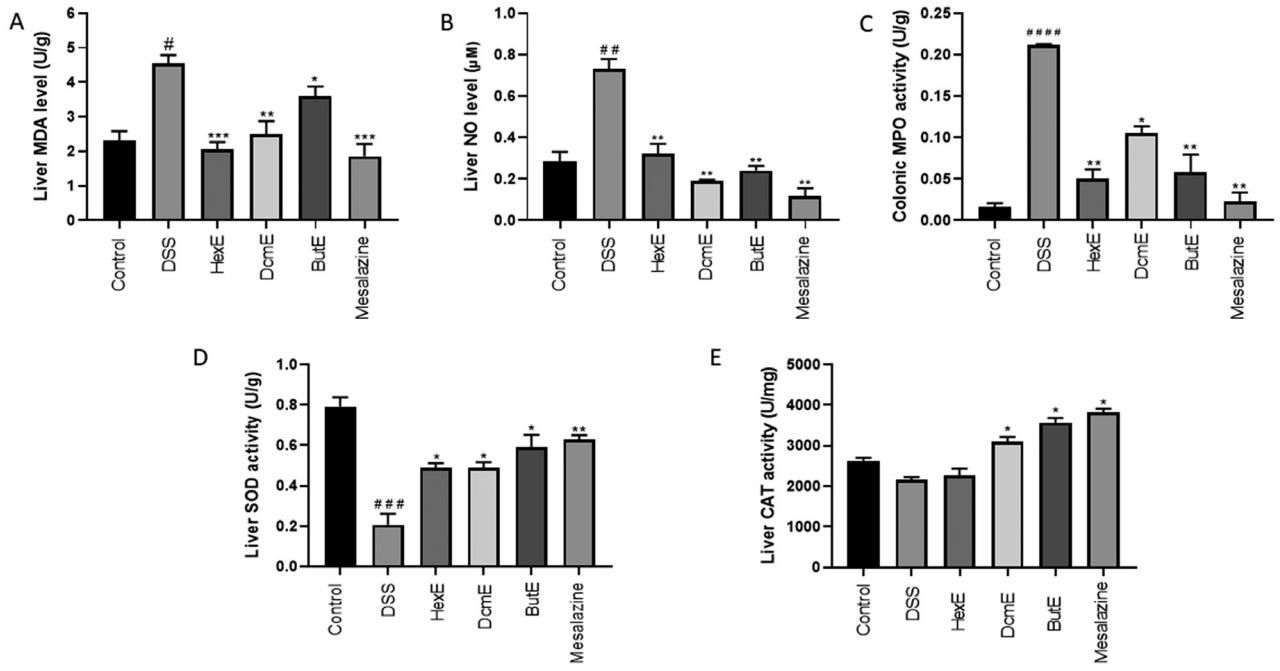

Figure 14 Effect of oxidative stress mediation. A–E, malondialdehyde (MDA), nitric oxide (NO), myeloperoxidase (MPO), superoxide dismutase (SOD) and catalase (CAT) levels of dextran sulfate sodium (DSS) induced and normal mice after HexE, DcmE and ButE administration. Data represented as the mean ± SD ($n = 6$). #$P < 0.05$ versus control group, ##$P < 0.01$ versus control group, ###$P < 0.001$ versus control group, ####$P < 0.0001$ versus control group; *$P < 0.05$ versus DSS group, **$P < 0.01$ versus DSS group, ***$P < 0.001$ versus DSS group, ****$P < 0.0001$ versus DSS group.

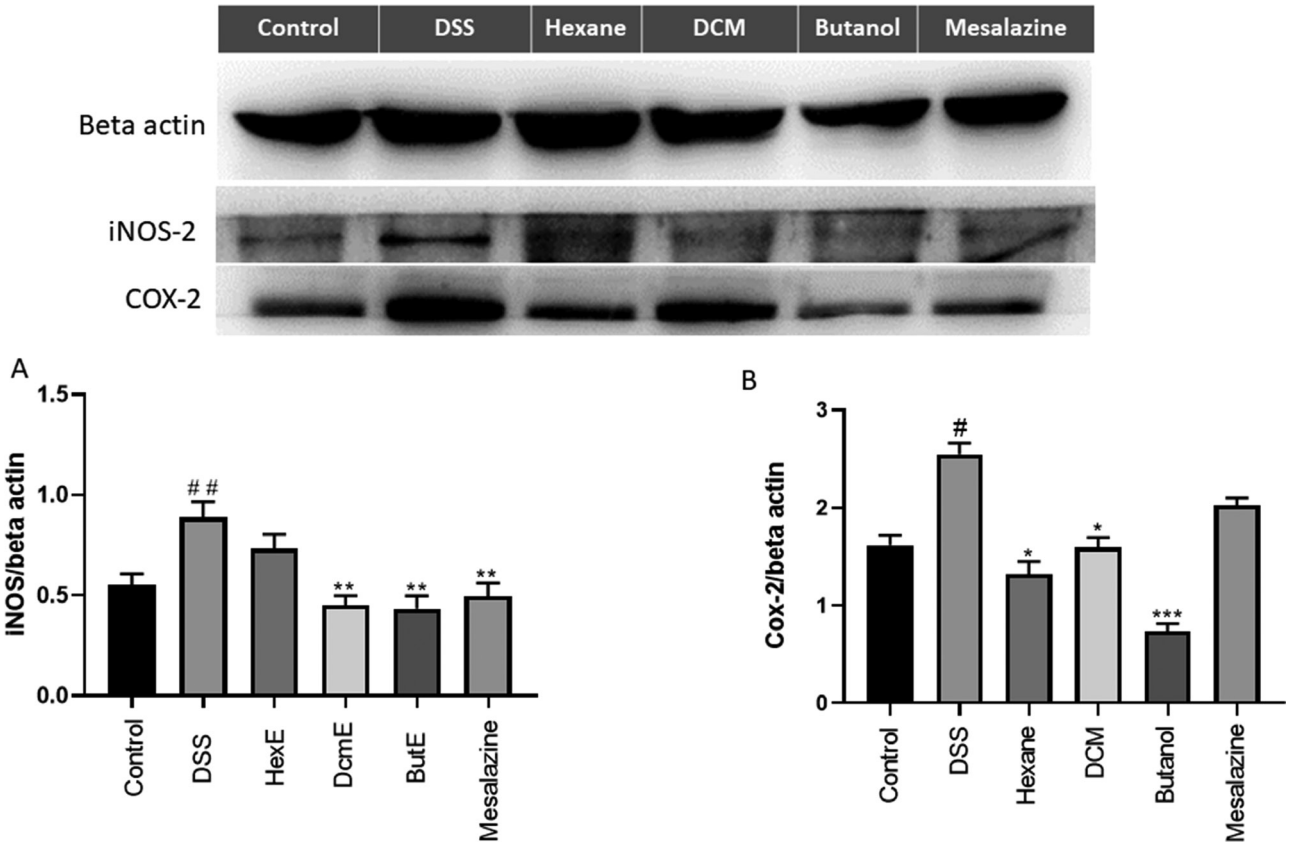

Figure 15 Effect of Hexane extract (HexE), dichloromethane extract (DcmE), butanol extract (ButE) on proteins Levels of inducible nitric oxide synthase (iNOS) (A) and cyclooxygenase-2 (COX-2) (B) were determined by western blot analysis. Representative blots from colon samples are shown and β actin was used as a loading control. Data represented as the mean ± SD ($n = 6$). #$P < 0.05$ versus control group, ##$P < 0.01$ versus control group; *$P < 0.05$ versus DSS group, **$P < 0.01$ versus DSS group, ***$P < 0.001$ versus DSS group.

Protein denaturation and DNA damage are the main ways for the ROS to induce cellular injury and necrosis. It is well-established fact that the intestinal inflammation and mucosal injury are directly related to the imbalance between antioxidants and pro-oxidants.[64] Oxidative stress is the outcome of the imbalance between the defence mechanism and ROS generation that ends up in free radical related pathologies.[65] Inflammation is an indispensable consequence of oxidative stress. In the current study, the activity of both antioxidant and pro-oxidants were evaluated and our experimental material maintained their balance compared to normal and model group. We analyzed the levels of CAT, SOD, MPO, MDA, ROS and NO. Due to the overproduction of ROS, the proper functions of antioxidants and pro-oxidants halts. These, in turn, starts a chain reaction to disrupt the normal physiological processes and changes the status of those enzymes responsible for maintaining the homeostasis of the gut.[66] Our findings suggested that *G. ellipticum* extracts, especially ButE, restored the level of those enzymes and eventually maintains gut homeostasis.

The imbalance of those enzymes and the consequent inflammation activates the signalling pathways by producing a significant amount of proinflammatory cytokines as well as disrupting the production of anti-inflammatory cytokines.[67] These trigger an inflammatory cascade that ends up in large aggregation of neutrophils in the colonic tissue resulting in tissue damage and subsequent complications.[68, 69] RT-PCR results of our experiment showed that the levels of proinflammatory cytokines significantly reduced which in turn prevents activation of NF-κB in all three-extract groups. MAPK cascade is an important signalling pathway of eukaryotes with several distinct subfamilies. Among them, c-Jun amino (N)-terminal kinases 1/2/3 (JNK1/2/3) and p38MAPK are very pivotal as they are triggered by several factors including stress, shock, cytokines and chemokines.[70] Activation of MAPKs components may be independent of each other but they all end up with similar outcomes, which is NF-κB activation and upregulation of COX-2 and iNOS.[71, 72]. The debate is still up about the precise mechanism of NF-κB modulation of MAPKs, but it may be by blocking the transactivation of NF-κB in the first place by phytochemicals to prevent inflammation and the consequent complications.[73] Our WB result lowered COX-2 and iNOS expression significantly by *G. ellipticum* extracts that were elevated by DSS treatment.

In conclusion, we explored the ameliorative effects of *G. ellipticum* extracts in both cellular and mouse model. Our result suggested that the protective effects of *G. ellipticum* extracts are associated with the reduction of DAI score, attenuation of histological damage, restoration of antioxidants and pro-oxidants and blocking of NF-κB pathway. These data strongly suggest that *G. ellipticum* extracts can be a potential source of medication for the possible treatment of IBD in the future that needs exploration. Similar to the cases of tormentil extracts, wormwood extract, green chiretta extract, mastic gum and *Aloe vera* gel. All of these already used in clinical trials to treat IBD and proved promising, even some were superior to mesalazine.[74, 75]

Author Contributions

Imam Hossen designed the study and performed the research; Rifat Nowshin Raka performed the research; Wu Hua, Cao Yanping, Chengtao Wang and Xiao Junsong were involved in all the steps of the study, resourcing and paper writing with everyones cooperation; Ashbala Shakoor analyzed the samples by UHPLC-Q-TOF-MS/MS; Arshad Mehmood, Song Jingyi, Jin Jian-Ming, and Xu Min were involved in sample preparation and processing.

Funding

The current work was supported by The National Key Research and Development Program of China (2016YFD0400801), Beijing municipal education commission general project (KM202010011010), Support Project of High-level Teachers in Beijing Municipal Universities (IDHT20180506), National Key Research and Development Program of China (2017YFC1600605), Beijing First Class Specialty Construction Project (PXM2019_014213_000010).

Conflict of interest

There are no conflicts of interest to declare.

References

1. Ye Y, Pang Z, Chen W *et al*. The epidemiology and risk factors of inflammatory bowel disease. *Int J Clin Exp Med* 2015; 8: 22529.
2. Ng SC, Shi HY, Hamidi N *et al*. Worldwide incidence and prevalence of inflammatory bowel disease in the 21st century: a systematic review of population-based studies. *Lancet* 2017; 390: 2769–78.
3. Alatab S, Sepanlou SG, Ikuta K *et al*. The global, regional, and national burden of inflammatory bowel disease in 195 countries and territories, 1990–2017: a systematic analysis for the Global Burden of Disease Study 2017. *Lancet Gastroenterol Hepatol* 2020; 5: 17–30.
4. Rodriguez-Canales M, Jimenez-Rivas R, Canales-Martinez MM *et al*. Protective effect of Amphipterygium adstringens extract on dextran sulphate sodium-induced ulcerative colitis in mice. *Mediators Inflamm* 2016; 2016: 1–12.
5. Torres J, Danese S, Colombel JF. New therapeutic avenues in ulcerative colitis: thinking out of the box. *Gut* 2013; 62: 1642–52.
6. Friswell M, Campbell B, Rhodes J. The role of bacteria in the pathogenesis of inflammatory bowel disease. *Gut Liver* 2010; 4: 295.
7. Khan I, Ullah N, Zha L *et al*. Alteration of gut microbiota in Inflammatory Bowel Disease (IBD): cause or consequence? IBD treatment targeting the gut microbiome. *Pathogens* 2019; 8: 126.
8. Rezaie A, Parker RD, Abdollahi M. Oxidative stress and pathogenesis of inflammatory bowel disease: an epiphenomenon or the cause? *Dig Dis Sci* 2007; 52: 2015–21.
9. Roessner A, Kuester D, Malfertheiner P *et al*. Oxidative stress in ulcerative colitis-associated carcinogenesis. *Pathol Res Pract* 2008; 204: 511–24.
10. Aviello G, Knaus UG. ROS in gastrointestinal inflammation: rescue or sabotage? *Br J Pharmacol* 2017; 174: 1704–18.
11. Schneider MJ, Abdel-Aziz H, Efferth T. Phytochemicals for the treatment of inflammatory bowel diseases. *Phytochem Rev* 2014; 13: 629–42.
12. Yahfoufi N, Alsadi N, Jambi M *et al*. The immunomodulatory and anti-inflammatory role of polyphenols. *Nutrients* 2018; 10: 1618.
13. Zaidi D, Wine E. Regulation of nuclear factor kappa-light-chain-enhancer of activated B Cells (NF-κβ) in inflammatory bowel diseases. *Front Pediatr* 2018; 6: 317.
14. Ordas I, Eckmann L, Talamini M *et al*. Ulcerative colitis. *Lancet* 2012; 38: 1606–19.
15. Park SC, Jeen YT. Current and emerging biologics for ulcerative colitis. *Gut Liver* 2015; 9: 18.
16. Capasso R, Orlando P, Pagano E *et al*. Palmitoylethanolamide normalizes intestinal motility in a model of post-inflammatory accelerated transit: involvement of CB 1 receptors and TRPV 1 channels. *Br J Pharmacol* 2014; 171: 4026–37.
17. Saxena A, Kaur K, Hegde S *et al*. Dietary agents and phytochemicals in the prevention and treatment of experimental ulcerative colitis. *J Tradit Complement Med* 2014; 4: 203–17.
18. Algieri F, Rodriguez-Nogales A, Rodriguez-Cabezas ME *et al*. Botanical drugs as an emerging strategy in inflammatory bowel disease: a review. *Mediators Inflamm* 2015; 2015: 179616.
19. Pagano E, Capasso R, Piscitelli F *et al*. An orally active cannabis extract with high content in cannabidiol attenuates chemically-induced intestinal

inflammation and hypermotility in the mouse. *Front Pharmacol* 2016; 7: 341.
20. Ganji-Arjenaki M, Rafieian-Kopaei M. Phytotherapies in inflammatory bowel disease. *J Res Med Sci* 2019; 24: 42.
21. Pagano E, Romano B, Iannotti FA *et al*. The non-euphoric phytocannabinoid cannabidivarin counteracts intestinal inflammation in mice and cytokine expression in biopsies from UC pediatric patients. *Pharmacol Res* 2019; 149: 104464.
22. Rogler G. Gastrointestinal and liver adverse effects of drugs used for treating IBD. *Best Pract Res Clin Gastroenterol* 2010; 24: 157–65.
23. Annaházi A, Molnár T. Optimal endpoint of therapy in IBD: an update on factors determining a successful drug withdrawal. *Gastroenterol Res Pract* 2015; 2015: 832395.
24. Voskuil MD, Bangma A, Weersma RK *et al*. Predicting (side) effects for patients with inflammatory bowel disease: the promise of pharmacogenetics. *World J Gastroenterol* 2019; 25: 2539.
25. Yang N, Xia Z, Shao N *et al*. Carnosic acid prevents dextran sulfate sodium-induced acute colitis associated with the regulation of the Keap1/Nrf2 pathway. *Sci Rep* 2017; 7: 1–12.
26. Yang G, Bibi S, Du M *et al*. Regulation of the intestinal tight junction by natural polyphenols: a mechanistic perspective. *Crit Rev Food Sci Nutr* 2017; 57: 3830–9.
27. Hossen I, Hua W, Ting L *et al*. Phytochemicals and inflammatory bowel disease: a review. *Crit Rev Food Sci Nutr* 2020; 60: 1321–45.
28. Jawarkar SV, Jat R. Invitro anti-inflammatory activity of Ethanol Extract of *Glochidion ellipticum*. *Current Pharm Res* 2015; 6: 1678.
29. Karande AM, Kamble HV, Kumbhar VH *et al*. Preliminary phytochemical screening of Glochidion ellipticum. *Euro J Exp Bio* 2016; 6: 41–5.
30. Jawarkar SV, Kane SR. Phytochemical and anthelmintic investigation of leaves of *Glochidion ellipticum* Linn. *Eur Exp Biol* 2017; 7: 9.
31. Sandhya S, Chaintanya RS, Vinod KR *et al*. An updated review on the genus Glochidion plant. *Arch Appl Sci Res* 2010; 2: 309–22.
32. Kane SR, Jawarkar S. Anthelmintic activity of extracts of Glochidion ellipticum Linn. *Indo Am J Phar Sci* 2017; 4: 4778–80.
33. Suradej B, Sookkhee S, Panyakaew J *et al*. Kaempferia parviflora extract inhibits STAT3 activation and interleukin-6 production in HeLa cervical cancer cells. *Int J Mol Sci* 2019; 20: 4226.
34. Ma F, Cui Q, Bai G. Combining UPLC/Q-TOF-MS/MS with biological evaluation for NF-κB inhibitors in uyghur medicine Althaea rosea flowers. *Front Plant Sci* 2019; 9: 1975.
35. Soonthornsit N, Pitaksutheepong C, Hemstapat W *et al*. In vitro anti-inflammatory activity of *Morus alba* L. stem extract in LPS-stimulated RAW 264.7 cells. *Evid Based Complement Alternat Med* 2017; 2017: 1–8.
36. Lee AY, Choi JW, Yokozawa T *et al*. Preventive effect of oligonol on nitric oxide and reactive oxygen species production through regulation of nuclear factor kappa B signaling pathway in RAW 264.7 macrophage cells against sodium nitroprusside. *RSC Adv* 2019; 9: 3987–93.
37. Chassaing B, Aitken JD, Malleshappa M *et al*. Dextran sulfate sodium (DSS)-induced colitis in mice. *Curr Protoc Immunol* 2014; 104: 15–25.
38. Sánchez-Fidalgo S, Cárdeno A, Villegas I *et al*. Dietary supplementation of resveratrol attenuates chronic colonic inflammation in mice. *Eur J Pharmacol* 2010; 633: 78–84.
39. Mehmood A, Zhao L, Wang C *et al*. Stevia residue extract alone and combination with allopurinol attenuate hyperuricemia in fructose–PO-induced hyperuricemic mice. *J Food Biochem* 2019; 44: e13087.
40. Tong LC, Wang Y, Wang ZB *et al*. Propionate ameliorates dextran sodium sulfate-induced colitis by improving intestinal barrier function and reducing inflammation and oxidative stress. *Front Pharmacol* 2016; 7: 253.
41. Hamesch K, Borkham-Kamphorst E, Strnad P *et al*. Lipopolysaccharide-induced inflammatory liver injury in mice. *Lab Anim* 2015; 49: 37–46.
42. Kim SH, Lee W, Kwon D *et al*. Metabolomic analysis of the liver of a dextran sodium sulfate-induced acute colitis mouse model: implications of the gut–liver connection. *Cells* 2020; 9: 341.
43. Peng Y, Hu K. Effect of garlic on rats with chronic intermittent hypoxia combined with diabetes mellitus. *Mol Med Rep* 2018; 17: 6174–84.
44. Zhang G, Zhu J, Zhou Y *et al*. Hesperidin alleviates oxidative stress and upregulates the multidrug resistance protein 2 in isoniazid and rifampicin-induced liver injury in rats. *J Biochem Mol Toxicol* 2016; 30: 342–9.
45. Chen W, Su H, Xu Y *et al*. In vitro gastrointestinal digestion promotes the protective effect of blackberry extract against acrylamide-induced oxidative stress. *Sci Rep* 2017; 7: 1–11.
46. Cho JY, Kim HY, Kim SK *et al*. β-Caryophyllene attenuates dextran sulfate sodium-induced colitis in mice via modulation of gene expression associated mainly with colon inflammation. *Toxicol Rep* 2015; 2: 1039–45.
47. Gao Z, Wu H, Zhang K *et al*. Protective effects of grape seed procyanidin extract on intestinal barrier dysfunction induced by a long-term high-fat diet. *J Funct Foods* 2020; 64: 103663.
48. Sadhu A, Moriyasu Y, Acharya K *et al*. Nitric oxide and ROS mediate autophagy and regulate Alternaria alternata toxin-induced cell death in tobacco BY-2 cells. *Sci Rep* 2019; 9: 1–14.
49. Naik E, Dixit VM. Mitochondrial reactive oxygen species drive proinflammatory cytokine production. *J Exp Med* 2011; 208: 417–20.
50. Kamalian A, Asl MS, Dolatshahi M *et al*. Interventions of natural and synthetic agents in inflammatory bowel disease, modulation of nitric oxide pathways. *World J Gastroenterol* 2020; 26: 3365.
51. Wan P, Chen H, Guo Y *et al*. Advances in treatment of ulcerative colitis with herbs: from bench to bedside. *World J Gastroenterol* 2014; 20: 14099.
52. Wilhelm SM, Love BL. Management of patients with inflammatory bowel disease: current and future treatments. *Clin Pharm* 2017; 83–92.
53. Vega RJS, Xolalpa NC, Castro AJA *et al*. Terpenes from natural products with potential anti-inflammatory activity. In: Perveen S, Al-Taweel A (eds.), *Terpenes and terpenoids*. London, UK: IntechOpen, 2018, 59–85.
54. Xiao HT, Wen B, Shen XC *et al*. Potential of plant-sourced phenols for inflammatory bowel disease. *Curr Med Chem* 2018; 25: 5191–217.
55. Wu H, Luo T, Li YM *et al*. Granny Smith apple procyanidin extract upregulates tight junction protein expression and modulates oxidative stress and inflammation in lipopolysaccharide-induced Caco-2 cells. *Food Funct* 2018; 9: 3321–9.
56. Oz HS, Chen T, de Villiers WJ. Green tea polyphenols and sulfasalazine have parallel anti-inflammatory properties in colitis models. *Front Immunol* 2013; 4: 132.
57. Marinovic MP, Morandi AC, Otton R. Green tea catechins alone or in combination alter functional parameters of human neutrophils via suppressing the activation of TLR-4/NFκB p65 signal pathway. *Toxicol In Vitro* 2015; 29: 1766–78.
58. Zhang H, Deng A, Zhang Z *et al*. The protective effect of epicatechin on experimental ulcerative colitis in mice is mediated by increasing antioxidation and by the inhibition of NF-κB pathway. *Pharmacol Rep* 2016; 68: 514–20.
59. Zhou K, Cheng R, Liu B *et al*. Eupatilin ameliorates dextran sulphate sodium-induced colitis in mice partly through promoting AMPK activation. *Phytomedicine* 2018; 46: 46–56.
60. Wen J, Khan I, Li A *et al*. Alpha-linolenic acid given as an anti-inflammatory agent in a mouse model of colonic inflammation. *Food Sci Nutr* 2019; 7: 3873–82.
61. Kang GD, Lim S, Kim DH. Oleanolic acid ameliorates dextran sodium sulfate-induced colitis in mice by restoring the balance of Th17/Treg cells and inhibiting NF-κB signaling pathway. *Int Immunopharmacol* 2015; 29: 393–400.
62. Pandurangan AK, Mohebali N, Esa NM *et al*. Gallic acid suppresses inflammation in dextran sodium sulfate-induced colitis in mice: possible mechanisms. *Int Immunopharmacol* 2015; 28: 1034–43.
63. Fang W, Zhu S, Niu Z *et al*. The protective effect of syringic acid on dextran sulfate sodium-induced experimental colitis in BALB/c mice. *Drug Dev Res* 2019; 80: 731–40.
64. Şengül N, Işık S, Aslım B *et al*. The effect of exopolysaccharide-producing probiotic strains on gut oxidative damage in experimental colitis. *Dig Dis Sci* 2011; 56: 707–14.
65. Valko M, Jomova K, Rhodes CJ *et al*. Redox-and non-redox-metal-induced formation of free radicals and their role in human disease. *Arch Toxicol* 2016; 90: 1–37.

66. Abraham C, Medzhitov R. Interactions between the host innate immune system and microbes in inflammatory bowel disease. *Gastroenterology* 2011; 140: 1729–37.
67. Strober W, Fuss IJ. Proinflammatory cytokines in the pathogenesis of inflammatory bowel diseases. *Gastroenterology* 2011; 140: 1756–67.
68. Neurath MF. Cytokines in inflammatory bowel disease. *Nat Rev Immunol* 2014; 14: 329–42.
69. Li YH, Adam R, Colombel JF *et al*. A characterization of pro-inflammatory cytokines in dextran sulfate sodium-induced chronic relapsing colitis mice model. *Int Immunopharmacol* 2018; 60: 194–201.
70. Pearson G, Robinson F, Beers Gibson T *et al*. Mitogen-activated protein (MAP) kinase pathways: regulation and physiological functions. *Endocr Rev* 2001; 22: 153–83.
71. Atreya I, Atreya R, Neurath MF. NF-κB in inflammatory bowel disease. *J Intern Med* 2008; 263: 591–6.
72. Sun P, Zhou K, Wang S *et al*. Involvement of MAPK/NF-κB signaling in the activation of the cholinergic anti-inflammatory pathway in experimental colitis by chronic vagus nerve stimulation. *PLoS One* 2013; 8: e69424.
73. Camacho-Barquero L, Villegas I, Sánchez-Calvo JM *et al*. Curcumin, a Curcuma longa constituent, acts on MAPK p38 pathway modulating COX-2 and iNOS expression in chronic experimental colitis. *Int Immunopharmacol* 2007; 7: 333–42.
74. Tang T, Targan SR, Li ZS *et al*. Randomised clinical trial: herbal extract HMPL-004 in active ulcerative colitis–a double-blind comparison with sustained release mesalazine. *Aliment Pharmacol Ther* 2011; 33: 194–202.
75. Triantafyllidi A, Xanthos T, Papalois A *et al*. Herbal and plant therapy in patients with inflammatory bowel disease. *Ann Gastroenterol* 2015; 28: 210.